AIP | Applied Physics Letters

Mixed conduction and grain boundary effect in lithium niobate under high pressure

Qinglin Wang, Cailong Liu, Yang Gao, Yanzhang Ma, Yonghao Han, and Chunxiao Gao

Citation: Applied Physics Letters **106**, 132902 (2015); doi: 10.1063/1.4916828
View online: http://dx.doi.org/10.1063/1.4916828
View Table of Contents: http://scitation.aip.org/content/aip/journal/apl/106/13?ver=pdfcov
Published by the AIP Publishing

Mixed conduction and grain boundary effect in lithium niobate under high pressure

Qinglin Wang,[1,2] Cailong Liu,[1] Yang Gao,[1,3] Yanzhang Ma,[3] Yonghao Han,[1,a)] and Chunxiao Gao[1,a)]

[1]*State Key Laboratory of Superhard Materials, Institute of Atomic and Molecular Physics, Jilin University, Changchun 130012, China*
[2]*Center for High Pressure Science and Technology Advanced Research, Changchun 130012, China*
[3]*Department of Mechanical Engineering, Texas Tech University, Lubbock, Texas 79409, USA*

(Received 8 February 2015; accepted 24 March 2015; published online 2 April 2015)

The charge transport behavior of lithium niobate has been investigated by *in situ* impedance measurement up to 40.6 GPa. The Li^+ ionic conduction plays a dominant role in the transport process. The relaxation process is described by the Maxwell-Wagner relaxation arising at the interfaces between grains and grain boundaries. The grain boundary microstructure rearranges after the phase transition, which improves the bulk dielectric performance. The theoretical calculations show that the decrease of bulk permittivity with increasing pressure in the *Pnma* phase is caused by the pressure-induced enhancement of electron localization around O atoms, which limits the polarization of Nb-O electric dipoles. © *2015 AIP Publishing LLC*. [http://dx.doi.org/10.1063/1.4916828]

Lithium niobate ($LiNbO_3$, LN) is a kind of important ferroelectric materials with many potential applications due to its good electro-optic, photorefractive, and nonlinear optical properties.[1–4] As the functional electro-optic materials, the conductive and dielectric properties of LN are determined by the creation, transportation, and recombination of charge carriers from the non-equilibrium to the equilibrium state. But different from the single crystal of LN, the polycrystals consist of many grain boundaries, and the transport properties are not only determined simply by the grains but also affected by the grain boundaries. Therefore, the polycrystalline may have some unique properties that would not be presented in the single crystals,[5] which is worth exploring.

The electric conductive and dielectric performance of LN are inextricably bound up with the types of the charge carriers (electrons or ions) and their scattering processes both in the grains and the grain boundaries. However, the above-mentioned issues have not been studied in detail. In this paper, we conduct an alternate-current (AC) impedance measurement of polycrystalline LN under high pressure up to 40 GPa to investigate the conduction mechanism involved in the charge transport process. The results show that both ionic and electronic conduction exist in LN, and the Li^+ ionic conduction plays a dominant role. The rearrangement of grain boundary microstructure can improve the bulk dielectric performance of LN. The first-principles calculations are also conducted for the better understanding of the electronic transport behavior of LN under compression.

A diamond anvil cell (DAC) with the culet diameter of 400 μm was utilized to generate high pressure. Impedance spectroscopy was measured with the double-plate electrodes that were integrated on the two diamond anvils. The experimental and theoretical calculation details can be found in the previous works.[6–8] The sample studied here was LN powder brought from Alfa Aesar Co. with a purity of 99.9995%.

The Nyquist representation of the impedance spectroscopy of LN under various pressures was shown in Fig. 1(a). As accepted for powdered sample, the equivalent circuit method is a reliable approach to describe the impedance spectra. In order to analyze the ionic conduction of Li^+, the

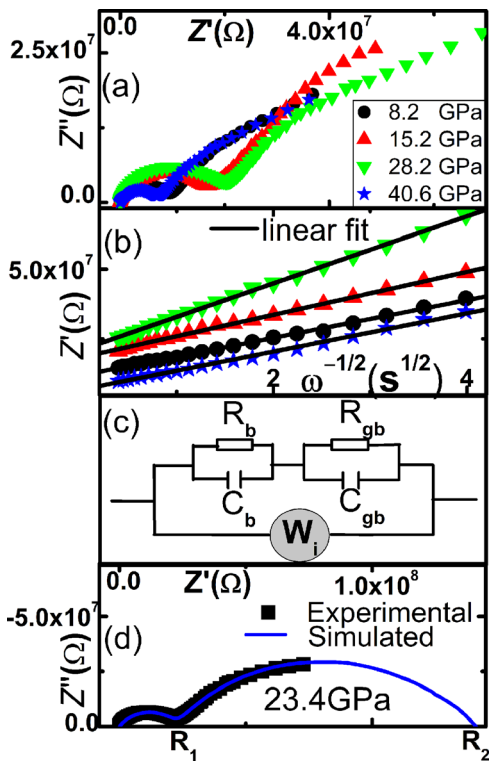

FIG. 1. (a) Nyquist impedance spectrum under various pressures. (b) The Z' vs $\omega^{-1/2}$ plots at low frequencies. (c) Circuit diagram equivalent to the conduction mechanism. The subscripts of the RC combinations are b for bulk, gb for grain boundary, and W_i denotes the Warburg impedance. (d) Nyquist-diagram at 23.4 GPa (data points). The continuous line represents the simulated spectra. R_1 and R_2 are two intercepts on the real impedance axis.

[a)]Authors to whom correspondence should be addressed. Electronic addresses: hanyonghao1978@aliyun.com and cc060109@qq.com.

Nyquist representation was replotted into a $Z' \sim \omega^{-1/2}$ plots as shown in Fig. 1(b). A linear relation between Z' and $\omega^{-1/2}$ was found in the low frequency region, indicating that there exists the diffusion of Li^+ ions through the grain boundaries at low frequencies. Thus, considering the ionic conduction, a Warburg impedance element to describe the diffusion of the Li^+ ions has been added to the equivalent circuit diagram [Fig. 1(c)]. The agreement of the simulated spectra with the experimental data [Fig. 1(d)] indicates the validity of considering the Li^+ ionic conduction in LN.

If more than one kind of charge carriers coexist in the materials, it is necessary to clarify which kind of carrier is dominant. The parameter for describing the contributions of one kind of carrier to the transport process is the transference number. In the case of LN, there are two kinds of charge carriers, Li^+ ions and the electrons. We define the transference number of Li^+ ion as t_i and electron as t_e.[9] According to the impedance spectra, we calculated the ionic and electronic transference number as shown in Fig. 2(b). It can be seen that in the whole pressure range, the dominant charge carriers in LN are Li^+ ions. In the *R*3*c* phase, the ionic transference number decreases with increasing pressure, while in the *Pnma* phase it increases.

From the impedance data, we can get the bulk dielectric constant using the following relation:

$$\varepsilon_b = C_b l/(\varepsilon_0 S), \tag{1}$$

where C_b is the bulk capacitance, S is the area of the electrode, l is the thickness of the sample, and ε_0 is the vacuum permittivity. The relaxation frequency of grains (f_b) can be obtained from the relationship of imaginary part Z'' versus frequency. The pressure dependent diffusion coefficient, bulk resistance, grain boundary resistance, bulk relaxation frequency, and bulk dielectric constant are shown in Fig. 2. For each parameter, a discontinuous change can be found at about 25.2 GPa. Because LN undergoes a phase transition from *R*3*c* to *Pnma* around 25 GPa,[10] the discontinuous change can be attributed qualitatively to the pressure-induced structural phase transition. These results show that the phase transition is accompanied by the detectable changes in the electrical transport behavior.

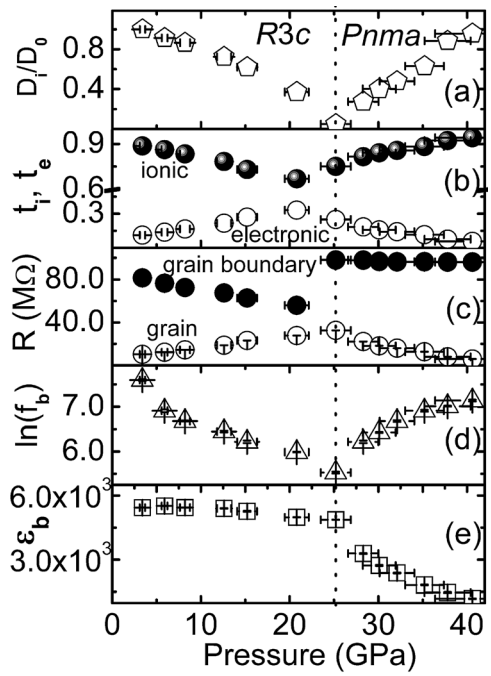

FIG. 2. Relationships of diffusion coefficient, transference number, bulk and grain boundary resistance, bulk relaxation frequency, and bulk dielectric constant versus pressure for LN. D_0 represents the diffusion coefficient at 3.4 GPa.

In the *R*3*c* phase, the Li^+ ions diffusion coefficient decreases with increasing pressure, while increases in the *Pnma* phase. This indicates that the grain boundary microstructure rearranged after the structural phase transition. In the *R*3*c* phase, the pressure makes the Li^+ ions diffusion through the boundaries more difficult, but the electronic transport easier [Figs. 2(a) and 2(c)]. In the *Pnma* phase, on the contrary, the pressure makes the Li^+ ions diffusion through the boundaries easier but has little effect on the electronic transport. The effect of pressure on diffusion coefficient in *R*3*c* and *Pnma* phases is attributed to the pressure-induced change in the ionic transference number.

The transport property of the electrons in LN depends on the scattering effect and the defect concentration of grain boundaries. As shown in Fig. 2(c), in the whole pressure range, the grain boundary resistance shows a relatively larger contribution to the total resistance, as compared to the bulk resistance, which indicates that the defects at grain boundaries dominate the electronic transport process. Below 25.2 GPa, the grain impedance increases with increasing pressure, which is caused by the following reasons: (i) The electron concentration keeps unchanged, but the defect energy level increases which results in the enhancement of the scattering effect. (ii) The defect energy level is fixed but the electron carrier concentration decreased, which is due to the bandgap broadening. We will discuss this issue later.

The combined usage of Z'' and M'' ($M^* = j\omega C_0 Z^*$) plots is particularly useful to understand the electronic transport behavior, since the Z'' plots highlight phenomena characterized by the large resistance, whereas the M'' plots identify the electrical responses with small capacitance.[11] The appearance and nature of Z'' peaks at a characteristic frequency provide the information of the type and strength of the dielectric relaxation. At all pressures, the Z'' curves have a relative weak peak at about 10^2–10^4 Hz.[9] The peak height increases with increasing pressure from 3.4 to 25.2 GPa and then decreases above 25.2 GPa, which is caused by the structural phase transition. Each curve is accompanied with a strong tail on the low frequency side. Similar phenomenon has also been observed in $CaCu_3Ti_4O_{12}$ (CCTO) reported by Liu *et al.*[12] Since the electronic response from grain boundary is associated with larger resistance, the response frequency is thus much lower than that of grains, which results in a relatively strong tail in the Z''-*f* plot. The weak responses in Z''-*f* are attributed to the grains and the strong responses are from the grain boundaries.

For an ideal Debye case, the Z'' and the imaginary modulus (M'') peaks of a particular *RC* component should be coincident on the frequency scale.[11] However, in our experiment, a significant mismatch between Z'' and M'' peaks can be found, and this can be attributed to the localized electronic conduction (here is the dipole relaxation for LN) in

the bulk sample.[13] Moreover, whether there is a peak in M''-f curve can be used to determine the electronic conduction mechanism in the grains (i.e., localized or non-localized process).[14] A peak appears in the entire pressure range, indicating that the electronic conduction type in the grains is localized and cannot be changed by pressure.

To gain a deeper insight into the energy exchange in the relaxation process, the complex dielectric behavior of LN has been investigated. In alternating-current impedance measurement, the molecular or atomic polarization by an applied electric field is time dependent. Because of the damping of the atoms motion in the dielectric, there is a delay of polarization corresponding to the change in field, which gives the dissipation factor tanδ, and is proportional to the energy absorbed per cycle by the dielectric from the field.[15]

The variation of the complex permittivity and the dielectric loss tangent with frequency under different pressures is shown in Figs. 3(a) and 3(b), respectively. In the high frequency region (>1 MHz), the ε'' increases with increasing frequency, accompanying the step decrease in ε'. This Debye-like relaxation (dipole relaxation) is so-called Maxwell-Wagner (M-W) relaxation and often occurs in the heterogeneous systems in which the component dielectrics have different conductivities. In polycrystalline LN material, there exist two heterogeneous dielectrics: the grains and the grain boundaries, in which the conductivities are different and therefore the system satisfies M-W condition. When electric current passes through the grain boundaries, the charges pile up at the boundaries and give rise to a Debye-like relaxation process under an external alternating field. At low frequency, the dipoles align themselves along the field and contribute fully to the total polarization. At higher frequency, the variation of the field is too rapid for the dipoles to align themselves, so their contribution to the polarization becomes negligible, leading to the decrease of ε' with increasing frequency.

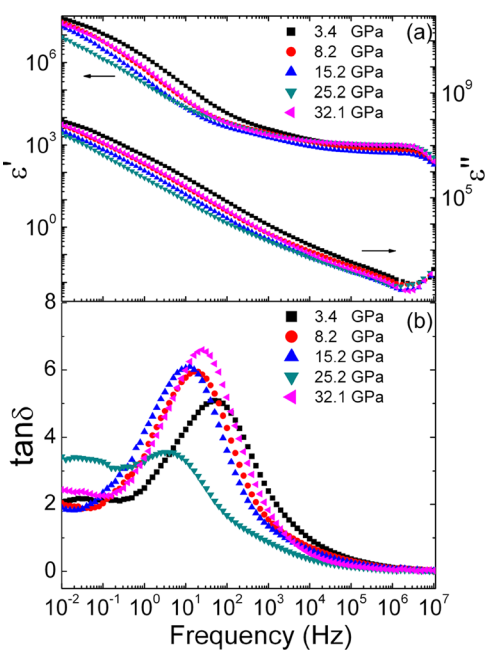

FIG. 3. Frequency dependence of (a) real and imaginary parts of permittivity and (b) tanδ for LN at different pressures.

The imaginary part of dielectric dispersion reflects the energy loss in LN caused by the electronic conduction and the relaxation process [Fig. 3(a)]. When frequency is less than 1 MHz, ε'' reduces linearly with increasing frequency, whereas the frequency is greater than 1 MHz, ε'' increased. This is a marked characteristic of the energy loss caused by the electronic conduction and the dipole relaxation, respectively. The observed dispersion of the permittivity implies that the hopping of electron carriers plays an important role among the localized states.[16] In the hopping process, the electron disorders its surroundings while its neighboring atoms move away from their equilibrium positions, causing the structural defects at the Nb sites of LN.[15] This has been reflected in the loss tangent curves [Fig. 3(b)], where well-defined peaks are observed. These peaks exhibit distributions of Debye-like relaxation processes and are consistent with the M-W relaxation model.[17–19]

The electron carrier transport in LN grains can be regarded as a charging process in a *RC* resonance circuit and the relaxation frequency actually denotes the charge-discharge rate of dipoles oscillation process, and its activation energy represents the energy to activate the resonance. The pressure dependent activation energy can be obtained by fitting the pressure dependence of bulk relaxation frequency in Fig. 2(d) to the differential form of Arrhenius equation

$$d(\ln f_b)/dP = -(1/k_B T)(dH/dP), \tag{2}$$

where H represents the activation energy, k_B is the Boltzmann constant, and T represents room temperature. The results are listed in Table SI, with the error less than 2%. It can be seen that the activation energy increases with increasing pressure in the $R3c$ phase, but decreases in the *Pnma* phase. This indicates that the pressure could make the charge-discharge processes in the $R3c$ phase of the LN more difficult, but make it much easier in the *Pnma* phase.

To obtain the pressure dependence of bandgap of LN, we performed band structure calculations. It is found that $d(lnR_b)/dP$ and dE_g/dP in each phase satisfy the Arrhenius relationship[9]

$$d(\ln R_b)/dP = (1/2k_B T)(dE_g/dP), \tag{3}$$

where R_b is the bulk resistance obtained from the experiments, E_g represents the bandgap obtained from band structure calculation, k_B is the Boltzmann constant, and T represents the room temperature. Above results indicate that the resistance increase in the $R3c$ phase is due to the bandgap's widening, while the resistance decrease in the *Pnma* phase results from the bandgap's narrowing. The pressure-induced variation in bandgap leads to the change of electron carrier concentration.

For achieving a proper understanding of the electron carrier transportation of LN, the difference charge density calculations have been conducted.[9] As the pressure increasing, the electron charge transfer happens from Nb^{5+} ion to O^{2-} ion in the *Pnma* phase, which causes an enhancement in electron localization around O atoms. Thus, the decrease of bulk relative permittivity in the *Pnma* phase is caused by the pressure-induced strengthening of electron localization

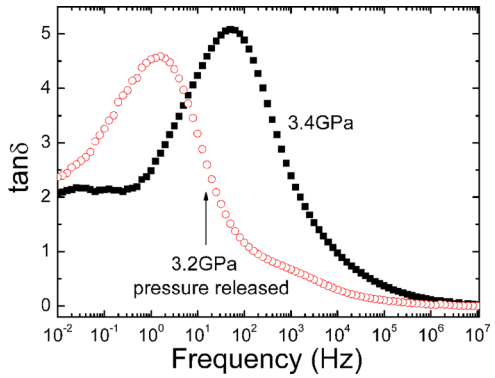

FIG. 4. Loss tangent of LN at 3.4 GPa and 3.2 GPa after pressure release.

around O atom, and the polarization of Nb-O electric dipoles becomes more difficult. In the *R*3*c* phase, the charge transfer is not pronounced and the bulk relative permittivity has almost no perceptible variation.

It should be noted that the compression has different effects on the polarization behavior of LN in *R*3*c* and *Pnma* phases. The loss tangent at 3.4 GPa and 3.2 GPa after pressure release is given in Fig. 4. Compared with the Z''-f peaks in grains, the corresponding frequency at the loss peak decreases about two orders of magnitude, thus the dielectric loss is mainly ascribed to the grain boundaries effects. When pressure is released to 3.2 GPa, the loss peak value decreases and the loss response frequency region narrows greatly, which indicates again that the grain boundary microstructure rearranges after the phase transition, and it does not go back to the initial state after the pressure release. In addition, after a pressure cycle, the dielectric loss in low frequency region has dropped considerably. Therefore, the dielectric performance of the material can be improved by modulating the grain boundary microstructure.

In summary, the pressure-induced electrical transport properties of $LiNbO_3$ have been investigated under pressure by *in situ* impedance measurement. The dominant transport carrier is Li^+ ions in the pressure range. The Debye-like relaxation can be explained by the Maxwell-Wagner relaxation arising at the interfaces between grain and grain boundary. Based on difference charge density calculations, the decrease of relative permittivity in the *Pnma* phase is caused by pressure-induced strengthening of electron localization around O atoms. The rearrangement of grain boundary microstructure after the phase transition makes the diffusion of Li^+ ions through the boundaries easier and improves the bulk dielectric performance of $LiNbO_3$. The idea of grain boundary design and control, i.e., the manipulation of polycrystalline dielectric performance through altering the grain boundary distribution, can be regarded as a promising approach to improve the bulk properties of materials.

This work was supported by the National Basic Research Program of China (Grant No. 2011CB808204), the National Natural Science Foundation of China (Grant Nos. 11374121, 11404133, and 11304034), China Postdoctoral Science Foundation (Grant No. 2013M540243), and Program of Science and Technology Development Plan of Jilin Province (Grant Nos. 20140520105JH and 201201106).

[1]D. Sando, E. Jaatinen, and F. Devaux, Appl. Opt. **48**, 4676 (2009).
[2]D. F. Xue and X. K. He, Phys. Rev. B **73**, 064113 (2006).
[3]R. K. Choubey, P. Sen, P. K. Sen, R. Bhatt, S. Kar, V. Shukla, and K. S. Bartwal, Opt. Mater. **28**, 467 (2006).
[4]O. Beyer, I. Breunig, F. Kalkum, and K. Buse, Appl. Phys. Lett. **88**, 051120 (2006).
[5]H. Y. Chang, S. Y. Cheng, and C. I. Sheu, Acta Mater. **52**, 5389 (2004).
[6]Y. H. Han, C. X. Gao, Y. Z. Ma, H. W. Liu, Y. W. Pan, J. F. Luo, M. Li, C. Y. He, X. W. Huang, G. T. Zou, Y. C. Li, X. D. Li, and J. Liu, Appl. Phys. Lett. **86**, 064104 (2005).
[7]C. Y. He, C. X. Gao, Y. Z. Ma, M. Li, A. M. Hao, X. W. Huang, B. G. Liu, D. M. Zhang, C. L. Yu, G. T. Zou, Y. C. Li, H. Li, X. D. Li, and J. Liu, Appl. Phys. Lett. **91**, 092124 (2007).
[8]Q. L. Wang, Y. H. Han, C. L. Liu, Y. Z. Ma, W. B. Ren, and C. X. Gao, Appl. Phys. Lett. **100**, 172905 (2012).
[9]See supplementary material at http://dx.doi.org/10.1063/1.4916828 for calculation method of transference numbers of ions and electrons, impedance Z'' and modulus M'' spectroscopic plots against frequency under different pressures, the pressure dependence of grain activation energy, $d(lnR_b)/dP$ obtained experimentally and dE_g/dP obtained theoretically, and calculated difference charge density maps through the Nb and O atoms.
[10]T. Mukaide, T. Yagi, N. Miyajima, T. Kondo, N. Sata, and T. Kikegawa, J. Appl. Phys. **93**, 3852 (2003).
[11]D. C. Sinclair and A. R. West, J. Appl. Phys. **66**, 3850 (1989).
[12]J. J. Liu, C. G. Duan, W. N. Mei, R. W. Smith, and J. R. Hardy, J. Appl. Phys. **98**, 093703 (2005).
[13]M. A. L. Nobre and S. Lanfredi, J. Appl. Phys. **93**, 5576 (2003).
[14]R. Gerhardt, J. Phys. Chem. Solids **55**, 1491 (1994).
[15]A. Dutta, T. P. Sinha, and S. Shannigrahi, Phys. Rev. B **76**, 155113 (2007).
[16]D. Adler and J. Feinleib, Phys. Rev. B **2**, 3112 (1970).
[17]O. Bidault, P. Goux, M. Kchikech, M. Belkaoumi, and M. Maglione, Phys. Rev. B **49**, 7868 (1994).
[18]N. Ortega, A. Kumar, R. S. Katiyar, and J. F. Scott, Appl. Phys. Lett. **91**, 102902 (2007).
[19]J. X. Zhang, J. Y. Dai, and H. L. W. Chan, J. Appl. Phys. **107**, 104105 (2010).